Available online at www.sciencedirect.com
ScienceDirect
Ceramics International 35 (2009) 2179–2184
CERAMICS INTERNATIONAL
www.elsevier.com/locate/ceramint

Microwave properties of chromium-substituted lithium ferrite

Yen-Pei Fu [a,*], Dung-Shing Hung [b], Yeong-Der Yao [c]

[a] Department of Materials Science and Engineering, National Dong-Hwa University, Shou-Feng, Hualien 974, Taiwan
[b] Department of Information & Telecommunications Engineering, Ming Chuan University, Taipei 111, Taiwan
[c] Department of Materials Engineering, Tatung University, Taipei 104, Taiwan

Received 16 September 2008; received in revised form 22 October 2008; accepted 27 November 2008
Available online 14 January 2009

Abstract

A structure characterization of chromium-substituted lithium ferrite specimens was carried out by the X-ray diffraction technique and found that the lattice parameter decreases with increasing of Cr-substitution content and the microstructure was determined by scanning electron microscopy (SEM), which revealed that the average grain size of chromium-substituted lithium ferrite decreases gradually with increasing Cr-substitution content.

The magnetic moments calculated from Neel's molecular field model are in agreement in the experiment result, which indicates that the saturation magnetization decreases monotonically with increasing Cr-substitution content. The values of saturation magnetization (Ms) for $Li_{0.5}Fe_{1.5-x}Cr_xO_4$ specimens decrease from 38.9 emu/g for $x = 0.0$ to 9.9 emu/g for $x = 1.0$. The microwave properties (complex permittivity and permeability) were measured in the 8–13 GHz frequency range by the cavity perturbation. The systematic variations of the real and imaginary parts of both permittivity and permeability with frequency and composition have been analyzed. The real and imaginary parts of both permittivity and permeability values decreased gradually with increasing frequency. The real part of permittivity ε' values are found to vary in the range of 15.44–12.37, and the real part of permeability μ' values are found to vary in the range of 3.95–1.27.

Keywords: A. Powders: solid state reaction; C. Dielectric properties; C. Magnetic properties; D. Spinels; E. Soft magnets

1. Introduction

Lithium ferrites are important components of microwave devices such as isolators, circulars, gyrators, and phase shifters and memory cores owing to their high Curie temperature, high saturation magnetization, and hysteresis loop properties, which offer performance advantage over other spinel structures [1–4]. The family of substituted lithium ferrites have attracted the attention of scientists for a long time and have been developed as a replacement for yttrium iron garnet (YIG) owing to their low cost [5]. Since the number of ferric ions on A and B sites is unequal in lithium ferrite, the calculated magnetic moment is not just that of lithium ions, but is given by the difference in the magnetic moment of ions on A and B sites. Consequently, lithium ferrite possesses a higher Curie temperature than other spinel ferrites [6]. $Li_{0.5}Fe_{2.5}O_4$ is an inverse spinel with the Li^+ and three-fifths of the Fe^{3+} ions occupying the octahedral B sites of the cubic spinel structure of the general formula AB_2O_4 [7]. Moreover, lithium ferrite have been also promising substitutes for Ni–Cu–Zn ferrites in advanced planar ferrite devices, because of their low sintering temperature, high Curie temperature and excellent electromagnetic properties at high frequency [8]. Because lithium ferrite has an important role in microwave devices, its performances of permeability and permittivity properties in the GHz frequency range is very important. Therefore, the purpose of the present paper is to study the complex permittivity and permeability properties of chromium-substituted lithium ferrite.

2. Experimental procedure

Chromium-substituted lithium ferrites ($Li_{0.5}Fe_{2.5-x}Cr_xO_4$) with $0.0 \leq x \leq 1.0$ were prepared following the conventional ceramic method. Samples were prepared from reagent-grade powders of Li_2CO_3, Cr_2O_3, and Fe_2O_3. Appropriate proportion of these compound were taken and ball-milled for 12 h in

* Corresponding author. Tel.: +886 3 863 4209; fax: +886 3 863 4200.
E-mail address: d887503@alumni.nthu.edu.tw (Y.-P. Fu).

0272-8842/$34.00
doi:10.1016/j.ceramint.2008.11.027

distilled water in order to mix them thoroughly and improved the homogeneity. The resulting mixtures were dried, and calcined at 700 °C for 4 h. Subsequently the whole mixture was remilled for 6 h and dried. The dried and sieved powder was pressed in the form of pellets using a small amount of PVA as binder with an applied uniaxial pressure of 1000 kgf/cm^2. The pellets sample were then finally sintered at 1200 °C for 4 h in air and furnace cooled.

Computerized X-ray powder diffraction (XRD, Rigaku D/Max-II, Tokyo, Japan) analysis, together with Cu K_α radiation with $\lambda = 0.15405$ nm was used to identify the crystalline phase and calculate lattice parameter. The morphological features of chromium-substituted lithium ferrite were observed using a scanning electron microscope (SEM; Hitachi S-3500H, Tokyo, Japan). A vibrating sample magnetometer (VSM, 7407 Lake Shore, Westerville, OH, USA) was used to measure the saturation magnetization (Ms) and intrinsic coercive force (Hc) of the calcined $Li_{0.5}Fe_{2.5-x}Cr_xO_4$ powders. Cavity perturbation has been used for the measurements of the complex permittivity and permeability of chromium-substituted lithium ferrite in the microwave frequencies. All the measurements were carried out at room temperature. The cavity used was made from the standard copper waveguide and rectangular cavity resonator with dimensions $L = 100$, $a = 28$, $b = 20$ mm, and the slot is 90 mm × 5 mm as shown in Fig. 1. The cavity was connected to a network analyzer (Agilent 8510C, Santa Clara, CA, USA) and excited into several modes. Thin chromium-substituted lithium ferrite slabs were placed straight through the slot in the cavity. Measurements and calculations were made according to the procedure described elsewhere [9–12].

3. Results and discussion

Unlike other spinel-type ferrites, lithium ferrite exists in two different crystalline forms. The α-phase has an FCC inverse spinel structure with space group of $P4_332$ and α-phase is an ordered phase in which the Li^+ and Fe^{3+} ions are ordered in the 1:3 ratio in the octahedral B sites of the cubic spinel structure, whereas the remaining Fe^{3+} ions occupy the tetrahedral A sites. Whereas the β-phase is a disordered phase where the Li^+ and Fe^{3+} ions are randomly distributed in the octahedral interstices and the space group is $Fd\bar{3}m$ [13–15]. In this study, XRD analysis has confirmed that the $Li_{0.5}Fe_{2.5-x}Cr_xO_4$ specimens contain only the α-phase. All the peaks in the pattern are matched well with JCPDS card (No. 38-0259). No β-phase is detected in the XRD patterns of samples. The presence of α-phase is due to the fact that during the usual ceramic method of synthesis of the bulk ferrite, a slow cooling process form above 755 °C yields the ordered phase. However, the disorder phase can be obtained by quenching from high temperatures. It is concluded that an order–disorder phase transition takes place in the temperature range 733–755 °C.

When doped with smaller Cr^{3+} ions, the spinel lithium ferrite will shrink. Doped Cr^{3+} ions in a spinel-type structure will induce uniform strain in the lattice as the material is elastically deformed. This effect causes the lattice plane spacing change and the diffraction peaks shift to a higher 2θ position. Generally, as the Cr-substitution content increases, the lattice constant decreases. It is due to the fact that different radii of Fe^{3+} (0.64 Å) and Cr^{3+} (0.62 Å) ions in an oxide solid solution with a spinel-type structure. Noticeably, the lattice parameter is nonlinearly dependent on Cr-substitution content for $Li_{0.5}Fe_{2.5-x}Cr_xO_4$. Gorter's defined the chemical formulas of $(Fe_{1.0})[Li_{0.5}Fe_{1.5}]O_4$ and $(Fe_{1.0-y}Li_y)[Li_{0.5-y}Fe_{1.5-x+y}Cr_x]O_4$ for $x = 0$ and $x > 0$, respectively. The formula for $x > 0$ indicates that Li^+ ions partially occupy the tetrahedral (A) site and that the distribution of Fe^{3+} ions occupying the tetrahedral (A) and octahedral [B] sites changes. y increases nonlinearly as x increases [16]. The observed nonlinear Cr-substitution content dependence of the lattice parameter may have resulted from the change of ion distribution.

The magnetization measurements for the $Li_{0.5}Fe_{2.5-x}Cr_xO_4$ specimens were carried out using a vibrating-sample magnetometer (VSM) at room temperature with an applied magnetic field of 10 kOe to reach saturation values. Introduction of Cr^{3+} ions into lithium ferrite greatly affects the magnetic properties. Fig. 2 plots the individually hysteresis loops for $Li_{0.5}Fe_{2.5-x}Cr_xO_4$ specimens. This figure indicates that the lithium ferrite

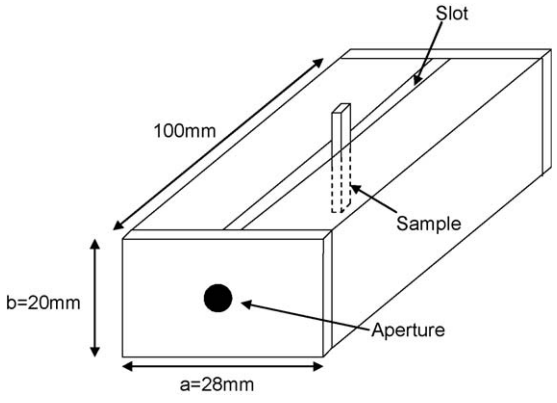

Fig. 1. Rectangular cavity resonator with dimensions $L = 100$, $a = 28$, and $b = 20$ mm. The slot is 90 mm × 5 mm, and the sample dimension is 15 mm × 5 mm × 1.5 mm.

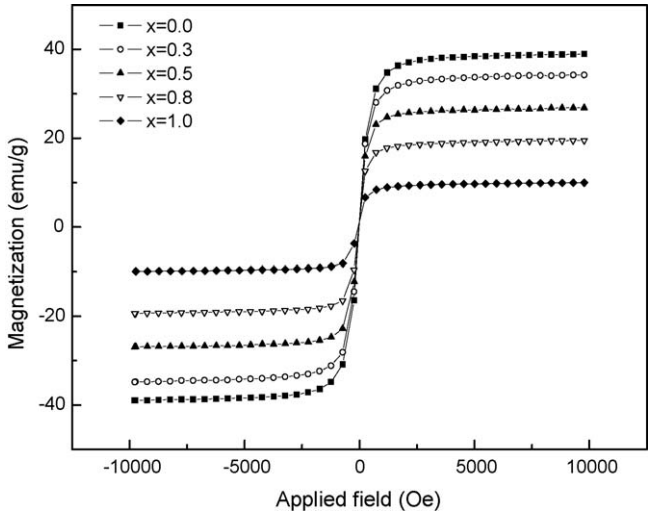

Fig. 2. Magnetization against applied field for $Li_{0.5}Fe_{2.5-x}Cr_xO_4$ powders.

Table 1
Magnetic properties of $Li_{0.5}Fe_{2.5-x}Cr_xO_4$ powder, an applied magnetic field of 10 kOe measured at room temperature.

Materials	Saturation magnetization (emu/g)	Coercive force (Oe)	Remanent magnetization (emu/g)
$x = 0.0$	38.9	10.6	1.21
$x = 0.3$	34.8	21.7	1.72
$x = 0.5$	26.9	17.7	1.25
$x = 0.8$	19.4	19.3	1.27
$x = 1.0$	9.9	49.5	1.17

is a soft magnetic material, which revealed minimal hysteresis. The main magnetic properties of $Li_{0.5}Fe_{2.5-x}Cr_xO_4$ powders are listed in Table 1.

The magnetic moment in ferrite is mainly due to the uncompensated electron spin of the individual ion and the spin alignments in the two sublattices which are arranged antiparallely. In a spinel ferrite, each ion at A site has 12 B-site ions as nearest neighbors. According to Neel's molecular field model [17], the AB super exchange interaction predominate the intrasublattice AA and BB interactions. Therefore, the net magnetic moment is given by the sum of the magnetic moments of A and B sublattices, i.e., $M = M_B - M_A$. In this study, the cationic distribution, Li^+ and Cr^{3+} ions are non-magnetic and do not contribute to the sublattice magnetization [18]. For chromium-substituted lithium ferrite, Li^+ substitution for Fe^{3+} ions at A site, leading to a decrease in the A site sublattice magnetization. Moreover, the Fe^{3+} ions are replaced by non-magnetic Li^+ and Cr^{3+} ions, leading to a decrease in the B site sublattice magnetization. Therefore, the magnetization of both sublattices decreases. The decrease of the B site magnetization is stronger than one of A site, which leads to a fall in the net magnetization. For example, we use the known magnetic moments for Li^+ ($0\mu_B$) and Fe^{3+} ($5\mu_B$).

For $Li_{0.5}Fe_{2.5}O_4$: $|M_s| = |M_B| - |M_A| = (0.5 \times 0 + 1.5 \times 5)\ \mu_B - (1 \times 5)\ \mu_B = 2.5\mu_B = 69.8\ Am^2/kg$. This value of magnetization is agrees well with the experimentally extrapolated value [19], thus proving the collinear nature of the pure ferrite. Using the cationic distribution of Cr^{3+}-substituted $Li_{0.5}Fe_{2.5}O_4$ and the fact that magnetic moment of Cr^{3+} is $3\mu_B$, the Neel's model leads to a fall in the net magnetization per formula unit.

For $Li_{0.5}Fe_{2.0}Cr_{0.5}O_4$: $|M_s| = |M_B| - |M_A| = (0.5 \times 0 + 1.0 \times 5 + 0.5 \times 3)\mu_B - (1 \times 5)\mu_B = 1.5\mu_B = 41.8\ Am^2/kg$. (In this formula, we supposed that all Cr^{3+} ions substituted for Fe^{3+} ions at the B-site.) This value is 40% lower than that of pure $Li_{0.5}Fe_{2.5}O_4$ calculated above. With increasing Cr^{3+} ions content in chromium-substituted lithium ferrite, the net magnetization decreased gradually. The magnetic moments calculated from Neel's molecular field model are in agreement in the experiment result, which indicates that the saturation magnetization decreases monotonically with increasing Cr-substitution content. The values of saturation magnetization (Ms) decrease from 38.9 ($Li_{0.5}Fe_{2.5}O_4$) to 9.9 emu/g ($Li_{0.5}Fe_{1.5}Cr_{1.0}O_4$). The coercive force (Hc) is an independent parameter, which can be altered by heat treatment or deformation and hence is not dependent on saturation magnetization. In this study, the coercive forces tend to rise in increasing Cr-substitution content, in which the values of coercive force varied in the range 10.6–49.5 Oe. The remanent magnetization (Mr) is also an independent parameter since it is not wholly dependent on saturation magnetization (Ms) and coercive force (Hc). The values of remanent magnetization varied in the range 1.17–1.72 emu/g.

In the microwave frequency region, the cavity perturbation is usually used for measurement of complex permittivity and permeability. This method is highly sensitive and only required a small quantity of specimen. The dispersive terms of a cavity are related to its resonance frequency and dissipative terms to its quality factors. An appropriate choice of cavity mode, which results the change in resonant frequency and quality factor can be used to calculate the complex permittivity ($\varepsilon' - j\varepsilon'$) and permeability ($\mu' - j\mu''$) of chromium-substituted lithium ferrite [20].

The variation of the real part and imaginary part of permittivity as function of microwave frequency at X-band, for chromium-substituted lithium ferrites were shown in Fig. 3. In the microwave frequency, the interfacial and dipolar polarization effects will be largely absent, the dielectric constant is mainly contributed by the atomic and electronic polarizations in ferrite grains. In Fig. 3(a), the real part of permittivity ε' value decreased gradually with increasing frequency from 8.09 to 12.37 GHz, which values are found to vary in the range 15.44–12.37. This is due to the fact that as the frequency of the microwave field increase above a certain frequency, the electronic exchange between Fe^{3+} and Fe^{2+} ions cannot follow the frequency of the alternating field [20]. In stoichiometric lithium ferrite, there are no Fe^{2+} ions. However the preparation of the ferrite requires high temperature sintering at 1200 °C for obtaining dense material. At such high temperature, oxygen dissociation and lithium volatility occurs resulting in formation of non-stoichiometric composition. The consequence is reduction of Fe^{3+} ions into Fe^{2+} ions [21]. The real part of permittivity ε' value also depended on stoichiometric composition, which ε' value decreased with increasing Cr-substitution content. The real part of permittivity ε' values of pure lithium ferrite is higher than chromium-substituted lithium ferrite, indicating that pure lithium ferrite have a higher number of Fe^{2+} ions and the number of Fe^{2+} ions decreased with increasing Cr-substitution content. With increased Cr-substitution content, the number of Fe^{2+} ions on the octahedral sites is decreased due to polarization in the microwave frequency. This behavior results in a continuous decrease in real part of permittivity ε' value. The minimum ε' value is found at $Li_{0.5}Fe_{1.5}Cr_{1.0}O_4$ specimen. This may be due to the presence of a lower number of Fe^{2+} in this composition. In Fig. 3(b), the imaginary part of permittivity ε'' value also found to decrease gradually with increasing frequency, which values are found to vary in the range of 0.29–0.04. The ε'' value is dependent of polarization, which value is proportional to polarization. If the sample have higher number of Fe^{2+} ions, this sample have higher polarization and ε'' value. This is due to the fact that Fe^{2+} ions can enhance hopping mechanism between Fe^{2+} and Fe^{3+}

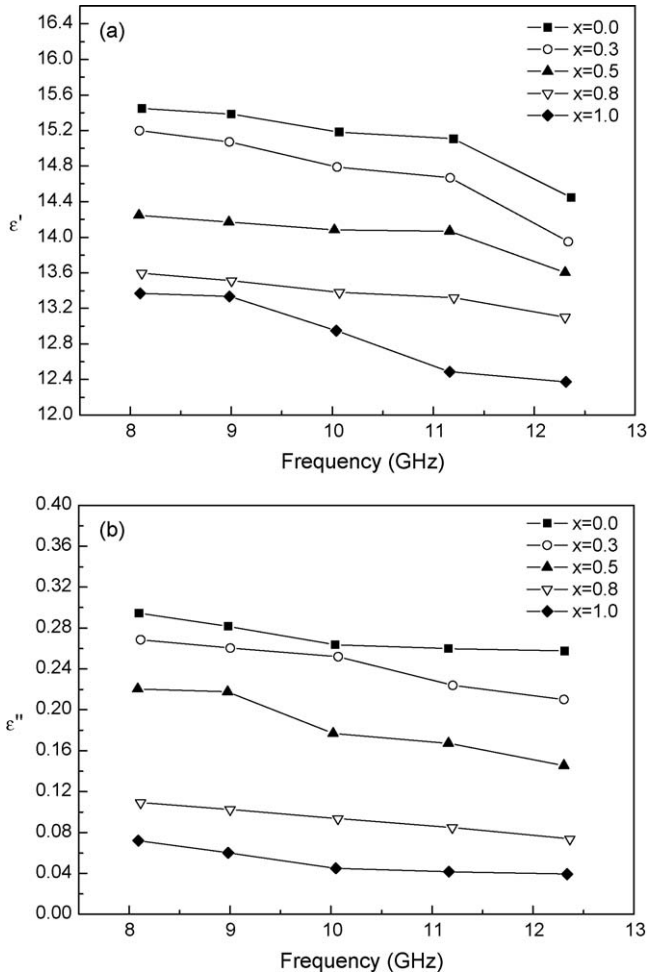

Fig. 3. The variation of (a) the real part and (b) the imaginary part of permittivity as a function of frequency (GHz) for $Li_{0.5}Fe_{2.5-x}Cr_xO_4$ ferrite sintered at 1200 °C for 4 h.

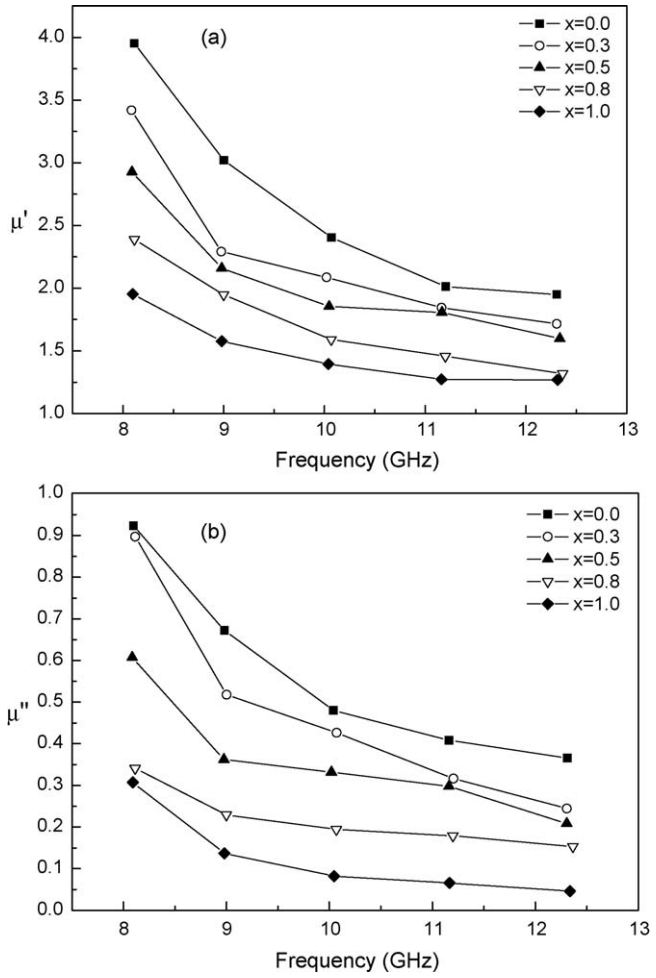

Fig. 4. The variation of (a) the real part and (b) the imaginary part of permeability as a function of frequency (GHz) for $Li_{0.5}Fe_{2.5-x}Cr_xO_4$ ferrite sintered at 1200 °C for 4 h.

ions present on equivalent crystallographic sites in the structure. It is concluded that the real part and imaginary part of permittivity values depended on the number of Fe^{2+} ions, and these values (ε' and ε'') revealed the same tendency in the microwave frequency at X-band.

Permeability of ferrite is mainly contributed by spin rotation and domain wall displacement in the microwave frequencies. When excited by an applied alternating magnetic field, the magnetization vector will precess around the anisotropy field. According to previous literatures [11,22], in the presence of an external RF field, the real part μ' can be expressed as follows:

$$\mu' = \left[\frac{\omega_P^2}{\omega_P^2 - \omega^2 + jd\omega}\right]\varepsilon\cos\omega t$$

where ω_p is the Larmor frequency, ω is the frequency of the alternating field, ε is the precessional angle, and $jd\omega$ is s damping term with d as the damping factor, which depends upon the damping of the precessional motion due to inhomogeneities and imperfections in the crystal lattice. When $\omega_p > \omega$, μ' increases gradually as ω increases. When $\omega_p = \omega$, a maximum μ' is obtained and when $\omega_p > \omega$, the magnetization vector and the RF magnetic field get out of phase, μ' suddenly falls and changes sign and become negative. This phenomenon is known as resonance. Resonance occurs when the frequency of the applied field coincides with the natural precessional frequency [23]. In Fig. 4(a), the real part of permeability μ' value decreased gradually with increasing frequency, which values are found to vary in the range of 3.95–1.27. This result is in accordance with Snoek's law, which equation can be defined by $f = (\gamma M_s/3\pi(\mu - 1))$[Hz], where f is the resonant frequency, Ms is saturation magnetization, and γ is gyromagnetic ratio. Above-mentioned formula indicates that as resonant frequency is low, the μ' value will be high. The real part of permeability μ' value significantly depended by saturation magnetization. According to above-mentioned magnetization result, with increasing Cr^{3+} ions amount in chromium-substituted lithium ferrite, the net magnetization decreased gradually. Therefore, the real part of permittivity μ' values of pure lithium ferrite is higher than chromium-substituted lithium ferrite. The microwave losses of magnetic nature are characterized by the imaginary part permittivity μ'' of the ferrite which exhibits a resonance behavior at angular frequency. The contributions to magnetic loss come from spin-lattice relaxation and magnetocrystalline anisotropy. The

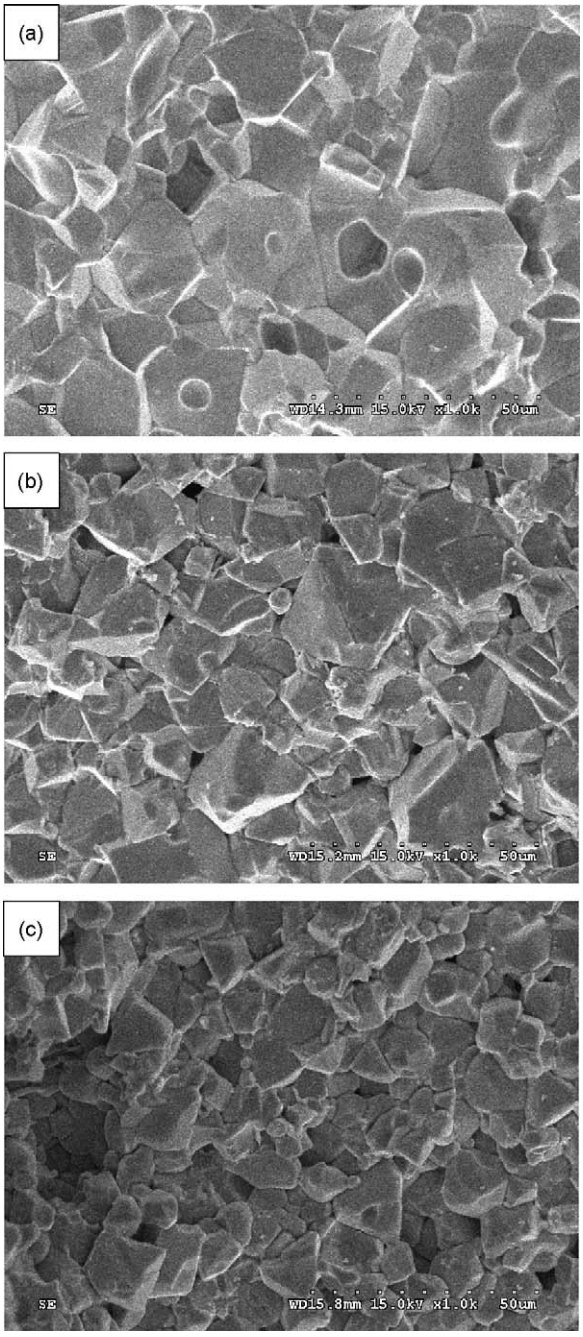

Fig. 5. Typical fracture microstructure of $Li_{0.5}Fe_{2.5-x}Cr_xO_4$ specimens for (a) $x = 0.0$, (b) $x = 0.5$ and (c) $x = 1.0$.

imaginary part of permeability μ'' as a function of frequency of $Li_{0.5}Fe_{2.5-x}Cr_xO_4$ specimens is shown in Fig. 4(b), reveling that the imaginary part permittivity μ'' values decreased gradually with increasing frequency at X-band. The permeability loss arises due to lag between the magnetization and applied alternating field. The imaginary part of permeability μ'' value decreased gradually with increasing frequency, which values are found to vary in the range of 0.92–0.04.

The microstructure such as grain sizes, grain morphology, densification, and precipitations, will significantly influence the dielectric and magnetic properties for chromium-substituted lithium ferrite. Fig. 5 illustrates the microstructure of $Li_{0.5}Fe_{2.5-x}Cr_xO_4$ specimens for $x = 0.0, 0.5$ and 1.0, respectively. The grain size significantly depended on the Cr-substitution content. The result reveals that the average grain size of chromium-substituted lithium ferrite decreases gradually with increasing Cr-substitution content. This indicates that addition with the chromium in lithium ferrite can hinder the grain growth and fine the grain size.

4. Conclusions

The effect of Cr-substitution content on the real and imaginary parts of both permittivity and permeability with frequency and composition for chromium-substituted lithium ferrite had been systematically studied. Experimental results revealed that the saturation magnetization decreases monotonically with increasing Cr-substitution content, the coercive force (Hc) is an independent parameter, which can be altered by heat treatment or deformation and hence is not dependent on saturation magnetization, the value of coercive forces tend to rise in increasing Cr-substitution content, the remanent magnetization is also an independent parameter since it is not wholly dependent on saturation magnetization and coercive force. The permittivity and permeability values depend on the frequency and stoichiometric composition. The real and imaginary parts of both permittivity and permeability values decreased gradually with increasing frequency in microwave region. The variation of complex permittivity may be due to the hopping mechanism between Fe^{2+} and Fe^{3+} ions. However, the variation of real and imaginary parts of and permeability depend on saturation magnetization and resonance behavior.

References

[1] H.M. Widatallah, C. Johnson, F. Berry, M. Pekala, Synthesis, structural, and magnetic characterisation of magnesium-doped lithium ferrite of composition $Li_{0.5}Fe_{2.5}O_4$, Solid State Commun. 120 (2001) 171–175.
[2] G.M. Argentina, P.D. Baba, Microwave lithium ferrite: an overview, IEEE Trans. Microwave Theory Technol. 22 (1974) 652–658.
[3] J.S. Baijal, S. Phanjoubam, D. Kothari, C. Prakash, P. Kishan, Hyperfine interactions and magnetic studies of Li–Mg ferrites, Solid State Commun. 83 (1992) 679–682.
[4] Y.P. Fu, C.S. Hsu, $Li_{0.5}Fe_{2.5-x}Mn_xO_4$ ferrite sintered from microwave-induced combustion, Solid State Commun. 134 (2005) 201–206.
[5] X. Qi, J. Zhou, Z. Yue, Z. Gui, L. Li, Permeability and microstructure of manganese modified lithium ferrite prepared by sol–gel auto-combustion method, Mater. Sci. Eng. B 99 (2003) 278–281.
[6] Y.P. Fu, Microwave-induced combustion synthesis of $Li_{0.5}Fe_{2.5-x}Cr_xO_4$ powder and their characterization, Mater. Res. Bull. 41 (2006) 809–816.
[7] S. Verma, P.A. Joy, Magnetic properties of superparamagnetic lithium ferrite nanoparticles, J. Appl. Phys. 98 (2005) 124312.
[8] Z. Yue, J. Zhou, X. Wang, Z. Gui, L. Li, Preparation and magnetic properties of titanium-substituted LiZn ferrites via a sol–gel auto-combustion process, J. Eur. Ceram. Soc. 23 (2003) 189–193.
[9] U. Raveendranath, K.T. Mathew, New cavity perturbation technique for measuring complex permeability of ferrite materials, Microwave Opt. Technol. Lett. 18 (1998) 241–243.
[10] M. Hajian, K.T. Mathew, L.P. Lighart, Measurement of complex permittivity with waveguide resonator using perturbation technique, Microwave Opt. Technol. Lett. 21 (1999) 269–272.
[11] A. Verma, D.C. Dube, Processing of nickel–zinc ferrite via the citrate precursor route for high-frequency applications, J. Am. Ceram. Soc. 88 (2005) 519–523.

[12] Y.P. Fu, C.W. Cheng, D.S. Hung, Y.D. Yao, Crystallization kinetics and microwave properties of $Bi_{0.5}Y_{2.5}Fe_5O_{12}$ via the coprecipitation process, J. Am. Ceram. Soc. 91 (2008) 155–159.
[13] S. Verma, J. Karande, A. Patidar, P.A. Joy, Low-temperature synthesis of nanocrystalline powders of lithium ferrite by an autocombustion method using citric acid and glycine, Mater. Lett. 59 (2005) 2630–2633.
[14] A. Tomas, P. Laruelle, J.L. Dormann, M. Nogues, Affinement de la structure des formes ordonnée et désordonnée de l'octaoxopentaferrate de lithium, $LiFe_5O_8$, Acta Crystallogr. C 39 (1983) 1615–1617.
[15] S.J. Marin, K. O'Keefe, D.E. Partin, Structures and crystal chemistry of ordered spinels: $LiFe_5O_8$, $LiZnNbO_4$, and Zn_2TiO_4, J. Solid State Chem. 113 (1994) 413–419.
[16] E.W. Gorter, Saturation magnetization and crystal chemistry of ferrimagnetic oxides. I and II. Theory of ferrimagnetism, Philips Res. Rep. 9 (1954) 295–320.
[17] B.D. Cullity, Introduction to Magnetic Materials, Addison-Wesley, MA, 1972, p. 141.
[18] M. Maisnam, S. Phanjoubam, H.N.K. Sarma, C. Prakash, L.R. Devi, O.P. Thakur, Magnetic properties of vanadium-substituted lithium zinc titanium ferrite, Mater. Lett. 58 (2004) 2412–2414.
[19] R.A. McCurrie, Ferromagnetic Materials: Structures and Properties, Academic Press, San Diego, 1994, p. 132.
[20] N. Gupta, M.C. Dimri, S.C. Kashyap, D.C. Dube, Processing and properties of cobalt-substituted lithium ferrite in the GHz frequency range, Ceram. Int. 31 (2005) 171–176.
[21] H.G. Belegers, J.L. Snoek, Gyromagnetic phenomena occurring with ferrites, Philips Tech. Rev. 11 (1950) 313–340.
[22] A.J. Moulson, J.M. Herbert, Electroceramics: Materials, Properties and Applications, Chapman & Hall, London, 1990, p. 247.
[23] V.R.K. Murthy, S. Sundaram, B. Viswanathan, Microwave Materials, Narosa Publishing House, New Delhi, 1994, p. 143.